Liftoff of a 190 mg Laser-Powered Aerial Vehicle: The Lightest Wireless Robot to Fly

Johannes James[1], Vikram Iyer[3], Yogesh Chukewad[1], Shyamnath Gollakota[2], Sawyer B. Fuller[1]

***Abstract*— To date, insect scale aerial robots have required wire tethers for providing power due to the challenges of integrating the required high-voltage power electronics within their severely constrained weight budgets. In this paper we present a significant milestone in the achievement of flight autonomy: the first wireless liftoff of a 190 mg aerial vehicle.**

Our robot is remotely powered using a 976 nm laser and integrates a complete power electronics package weighing a total of 104 mg, using commercially available components and fabricated using a fast-turnaround laser based circuit fabrication technique. The onboard electronics include a light-weight boost converter capable of producing high voltage bias and drive signals of over 200 V at up to 170 Hz and regulated by a microcontroller performing feedback control. We present our system design and analysis, detailed description of our fabrication method, and results from flight experiments.

I. INTRODUCTION

Honeybee-sized insect-scale aerial robots (≈100 mg) are well suited to a variety of applications benefiting from their small scale including environmental monitoring, agricultural support, and search and rescue. Since they were originally proposed as "gnat robots" in 1989 by Brooks and Flynn [1] and attempted in earnest by the Berkeley Micro Robotic Fly project starting in the early 2000s [2], progress toward truly autonomous insect scale robots has seen important milestones. These include the first lift greater than weight of a 100 mg robot [3], subsequent controlled flight [4], sensor integration [5], and expanded capabilities such as landing [6]. However, in the decade that has followed first liftoff, not one of these 100 mg robots has been able to fly without tiny wires to power and control it.

Realizing wireless flight requires solving three key challenges that arise from the small scale:

- Insect scale at < 200 mg discourages traditional forms of propulsion such as a propeller driven by electromagnetic coils because unfavorable physics scaling [7]. Instead, flapping wings driven by piezo-electric actuators are more efficient [8]. While piezo-driven robots have been successfully used for flight, they require high potentials over 200 V [3]. Generating the necessary voltage signals has so far required large electronic components with a prohibitive weight relative to insect-scale aerial payload capacity (e.g. [9] at 675 mg).
- Wireless flight requires an energy source to power the electronic and mechanical components. To date, the smallest high-drain (>10 C) batteries available are too heavy at 350 mg (GM300910, PowerStream Technology, Orem, Utah). The only currently viable alternative is a battery-free design.
- Finally, all the required digital processing has to be performed on the aircraft. Onboard computation that operates within the size, weight and power (SWaP) requirements is not only necessary to control the electronics and piezo driver, but also a basic requirement for truly autonomous insect robots capable of sensing and more complex functionality.

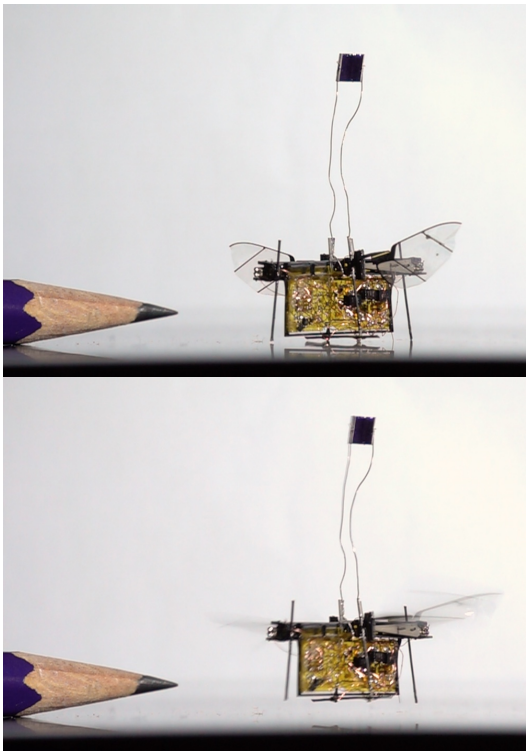

Fig. 1: (Top) The 190 mg RoboFly and power system before liftoff. (Bottom) After the laser is powered on, power reaches the robot through photovoltaic cell at top. Onboard electronics generate the waveform to drive the wings, causing the robot to lift off. After liftoff the robot is no longer in contact with its reflection on the surface below.

This paper demonstrates the lightest wireless robotic flight to date by showing the liftoff of a sub-200 mg aerial vehicle. To achieve this we introduce three key technical innovations. First, we present a novel ultra-lightweight and fast-turnaround circuit fabrication technique with which we

[1]Department of Mechanical Engineering, [2]Paul G. Allen School of Computer Science and Engineering, [3]Department of Electrical Engineering, University of Washington, Seattle, WA 98195. jmjames@uw.edu

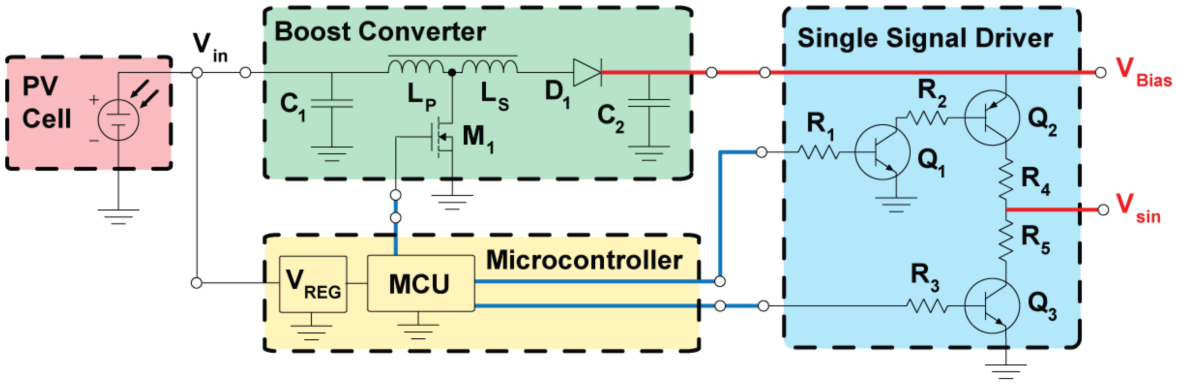

Fig. 2: Circuit schematic showing the complete power electronics system. The boost converter produces a high voltage bias (red) and the driver uses this to produce high voltage sinusoid. The boost converter and driver are controlled by PWM signals (blue) from the microcontroller.

create the first sub 100 mg boost converter and piezo driver that is integrated into an aerial robot. Second, we present a battery-free design by demonstrating the first wireless power transmission to an insect scale aerial robot at ranges of over 1 m using photovoltaic cells and lasers. Third, we demonstrate the first insect-scale aerial vehicle with onboard computation by integrating a light-weight microcontroller that we use to control the boost converter and piezo driver. Finally, we integrate all of these electronic components onboard an insect robot, constituting a 104 mg package, which is less than the weight of a typical toothpick. We use them to perform the first physically untethered flights of an insect-scale robot, weighing 190 mg altogether.

II. System Overview

Our bio-inspired insect robot consists of a dual wing flapping design driven by two piezoelectric actuators. Our full system capable of wireless takeoff begins with a laser source, which delivers a constant source of power wirelessly to the robot. A photovoltaic cell then converts the optical power to electrical power. The power provided by the laser is used to run the boost converter, driver, and microcontroller which produce sinusoidal voltage outputs capable of simultaneously driving the two piezo-electric actuators.

In the rest of the paper, we first describe our flight-weight power electronics which include our ultra light-weight boost converter and driver design, followed by a description of our rapid fabrication methods for producing the flight weight circuit and integrating an onboard microcontroller. Next we describe our laser system and the design choices for wireless power transfer. Finally, we present implementation details for our robofly followed by flight results.

III. Flight-Weight Power Electronics

The oscillating motion of the bimorph piezo beam actuators that flap the wings must be driven by a sinusoidal, high-voltage signal. This must be in the range of 200–300 V to maximize the power density produced by the actuator. The need for low weight and high efficiency strongly influence our design.

Efficiency would be improved if the actuator and wing assembly operated at both electrical and mechanical resonance. However, because the capacitance of the actuators is approximately 5 nF, an inductance needed to achieve electrical resonance at the flapping frequencies would be prohibitively heavy. Therefore, a design goal is that the sine wave should operate at a user-programmable frequency near the mechanical natural frequency of the actuator-wing system, 140–170 Hz [10].

We employ a design geared to bimorph actuators consisting of a constant, high-voltage bias signal and a sinusoidally varying signal channel, following the approach of [11]. An example signal appropriate for this configuration is shown at the top of Fig. 3.

A. Circuit design

Commercially available piezo driver ICs (e.g. Texas Instruments DRV2700) cannot produce the required voltage. Commercially-available integrated solutions such as the PD100 (Piezo Drive, Callaghan, Australia) are too heavy at 500 mg. While a monolithic SoC design is the typical solution for reducing the size and weight of electronics, we instead focus on a simple switched mode design built with off-the-shelf components.

This approach has a number of advantages. First, it allows for greater design flexibility and rapid prototyping which is important considering that insect robots are still an active area of research with frequent design changes. For example, optimizing an IC for a particular actuator design precludes further improvement in that domain or later incorporation of additional features such as energy recovery mechanisms. Second, designing a single SoC solution that integrates the high voltage actuator drive circuitry presents a design tradeoff. Digital circuits for processing can take advantage of device scaling to operate at low power and reduce size, however these devices cannot tolerant high voltages needed

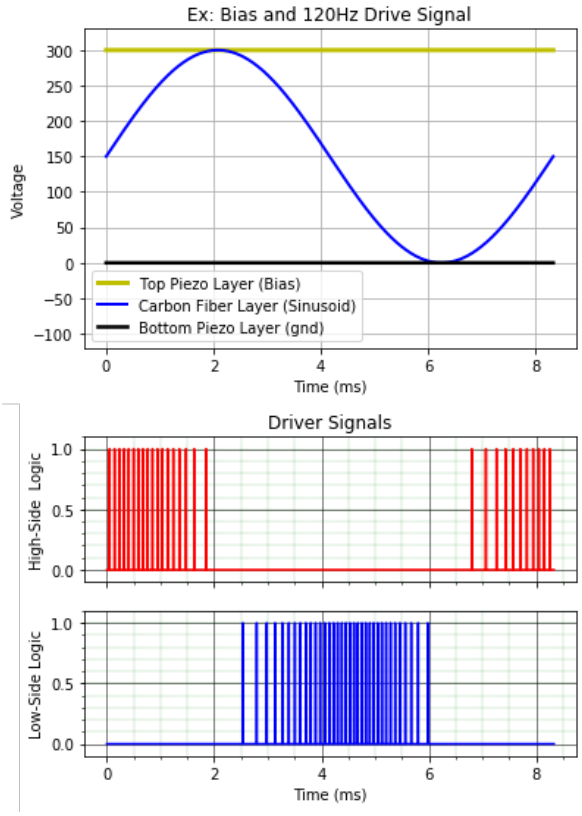

Fig. 3: (Top) Example target waveforms for boost converter output (yellow) and sinusoidal driver output signal(black); (Bottom) Example of driver pulse train varying by pulse frequency (PFM)

for the drive electronics. We instead choose to use a commercially available ARM microcontroller (STM32F051) to implement the timing and control which allows us to leverage the plethora of commercial products which are thoroughly tested and highly optimized for low power and size.

A schematic of our boost converter is shown in Fig. 2. The switching mode boost converter switches electrical current through a coupled inductor with a high turns ratio at frequencies above 100 kHz [11]. The switch control signal is generated by the pulse width modulation (PWM) output of a microcontroller and connected to the gate of the MOSFET M1 in Fig. 2. Current through the primary winding of the coupled inductors stores energy in the magnetic field which is transferred to the secondary winding. Brief high voltage pulses on the output of the secondary winding after the MOSFET switches rapidly to nonconducting state are rectified through a fast diode. The diode's output charges a high voltage capacitor for storage and this output is connected to the load. The load in this case is the driver circuit, which linearly regulates the center node of the bimorph actuator in order to drive sinusoidal displacement. The bias and driver waveforms seen in Fig. 4 are connected directly to the top piezo surface and the carbon fiber layer of both the bimorph actuators respectively.

The driver circuit is designed to source or sink current at a sinusoidal rate to the center node of the bimorph actuator

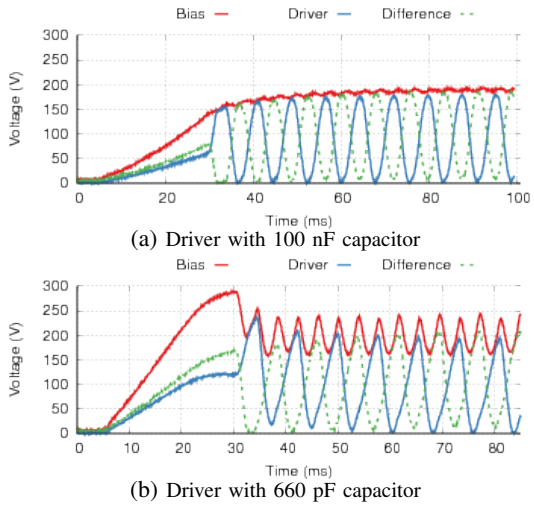

(a) Driver with 100 nF capacitor

(b) Driver with 660 pF capacitor

Fig. 4: Waveform output by onboard driver effecting modest amplitude sinusoid of controllable frequency by high-side and low-side control signals with a 100 nF capacitor on the bias rail in 4a and a 660 pF capacitor in 4b.

in simultaneous drive configuration. Transistors Q1 and Q2 are configured as a two stage amplifier designed to source current from the bias rail, implementing the "high side" to increase the sinusoid to its maximum voltage. Transistor Q3 generates the "low side" of the waveform by sinking current from the center node of each actuator to ground.

We use bipolar junction transistors (BJTs) as opposed to FETS standard in current aerial microrobotic research [12] simply due to the ability to tolerate higher voltages than FETs in somewhat smaller commercially available SMT packages, and simple gate biasing design for both linear operation and the rapid pulsing required for potential use of inductive energy recovery schemes [11]. Since the required sinusoid is at a low frequency compared to the clocks of microcontrollers, we generated the sinusoid using pulse width modulation, as depicted in Fig. 3. Since the microcontroller clock frequency is a significant factor in its power consumption, the frequency of the pulse width modulation was selected to generate a sufficiently smooth sinusoid with adequate PWM resolution, without excessively high internal oscillator frequency. Future work will investigate whether the DACs built into microcontrollers, PSoCs, FPGAs, or even passive oscillator circuits could generate the waveform in a way that improved efficiency.

Because actuator displacement depends on the voltage difference between the piezo layers and the center carbon fiber layer, our goal is to maintain a constant high voltage bias while the sinusoid varies over time. Dynamic common mode control of the bias rail as in [12] is desirable but must be conducted carefully so as to achieve the correct sinusoidal driver output which is effectively equal to $V_{bias} - V_{signal}$. The complications of common mode control are evident in Fig. 4b Because the actuator load varies dynamically during flight and the input power source may be unstable, we design a feedback controller to help regulate a constant bias voltage. We use a simple resistive voltage divider to

reduce the bias voltage to within the 3 V operating range of the microcontroller and use its ADC to digitize the value. Based on the ADC reading we adjust the duty cycle using a basic proportional controller in addition to feedforward terms anticipating dynamic load increases of the driver throughout the low frequency actuator cycle.

B. Circuit Performance

Fig. 4 shows the high voltage output waveforms generated by open-loop boost converter and driver for different storage capacitor values. As expected, a large 100 nF capacitor as shown in Fig. 4a produces a very consistent bias output thereby reducing the need for feedback control to maximize wing displacement. In contrast, the waveform with a smaller 660 pF capacitor varies noticeably, challenging feedback control and complicating the driving of consistent waveforms. While a large capacitor reduces bias variation it comes at a cost of 16 mg of weight. These waveforms also demonstrate two other important results. First, in both cases the circuit produces an amplitude greater than 170 V which we verified experimentally is the minimum required to lift our MAV. Second, the sinusoid waveform is smooth and does not have abrupt discontinuities that could potentially stress and damage the actuator.

IV. Circuit Fabrication Method

We fabricated the circuit described above with the smallest commercially available packages for each component with required characteristics. Although coupled inductors such as available in the Coilcraft LPR3015 series are similar to the needs of the boost converter, full control of component characteristics within a lower weight budget was obtained by custom manufacture in-house without great difficulty. Therefore, a coupled inductor with the required ratio of turns, inductance, winding series resistance, coupling, and total weight was custom built for the application and guided by simulation in order to optimize for operating conditions. We fabricated a custom inductor by winding 43 AWG wire around the ferrite core removed from an LPD3015 inductor for the primary side, and 46 AWG wire for the secondary. The wire used was selected due to availability, resistivity, insulation characteristics, and ease of winding for good magnetic coupling. Total component weight of the simple flyback transformer is 21 mg.

In addition to the size and weight of the components themselves, the circuit board and copper traces on which they are mounted contribute weight as well. Traditional PCB materials such as copper-clad FR4 have a density of 2.6 g/cm^3 which is not feasible for insect-scale applications. We instead developed a new rapid prototyping process for fabricating ultra light-weight circuits requiring no chemical etching. This process is an alternative to existing copper ablation flexible PCB fabrication techniques which are expensive and require care to ablate only the copper while leaving the substrate intact. Our process is inspired by the laser micro-machining methods used to fabricate the other parts of the insect robot, and uses the same equipment.

Fig. 5 outlines our fabrication process. We begin by cleaning both sides of a sheet of 25 μm copper foil with isopropanol and placing it on a low-tack adhesive (Gelpak X8, Hayward, CA). Next, we use the same UV DPSS laser micromachining system used for fabricating the actuators and body of the insect robot to cut out the desired copper traces. The 20 μm spot size of the laser has enough resolution for even the finest pitch electronic components.

After cutting, a low-power cleaning raster is performed to achieve better adhesion. We then peel the excess copper that can be peeled off of the Gelpak leaving only the desired pattern. Next, we place a piece of readily available 25 μm thick Kapton tape onto the copper and lift the traces off of the Gelpak. The result is a flexible circuit marginally thicker than 50 μm but still approximately 5-7 mg/cm^2 for a typical circuit design. We select Kapton tape as the substrate material due to its ability to withstand high temperatures needed for soldering. Thinner Kapton tape and copper sheet can be obtained, but is not as readily available. Such circuits are vulnerable to contamination at sites of exposed adhesive and are generally not as durable, but have in praxis survived repeated rework and handling in research applications.

The final step is to populate the circuit with components. While this can easily be done with a normal soldering iron for most components, the lightest weight microcontrollers available in wafer level chip scale (WLCSP) packages present a challenge. Because our circuit board only has a single side and used no soldermask or insulating layer to minimize weight, traces will short the contacts on the interior parts of the chip without care to avoid this. A simple method of addressing this is to precut holes in the kapton tape at the desired solder ball sites and align those holes to the circuit in the adhesion step. The chip is then aligned and placed on the reverse side and soldered at the desired contact points through the precut holes. Alternatively the same micro-machining method can be used to to cut an additional insulating layer of kapton that can be placed as a mask over the chip and allow the use of normal reflow soldering methods. The power electronics unit (PEU) of our insect robot was constructed in this fashion and the results at different points in the process can be seen in Fig.6.

V. LASER POWER TRANSFER

Achieving wireless liftoff requires powering all the above components. Our robot requires 200-300 mW of power for liftoff and requires a total of 25 mA of current.

The required energy density and peak current draw are beyond the capabilities of existing battery technologies, but a potential alternative is to use super-capacitors. A 7.5 mF capacitor for example has a maximum voltage of 2.6 V [13]. This voltage however is insufficient to run the boost converter even in simulation. A series parallel combination of 4 super-capacitors could theoretically provide power for 250 ms of flight at which point the capacitors would discharge from

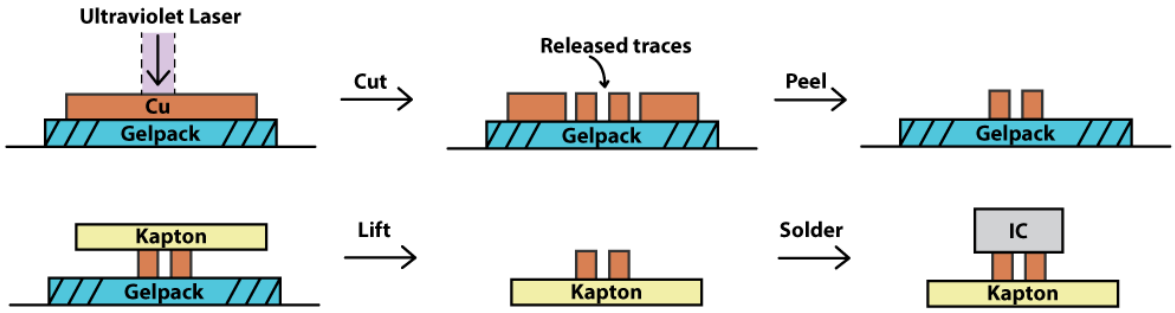

Fig. 5: Steps of the circuit fabrication process beginning with laser micro-machining, followed by removing the excess copper and adhering the desired traces to Kapton tape to produce an ultra-light weight flexible PCB.

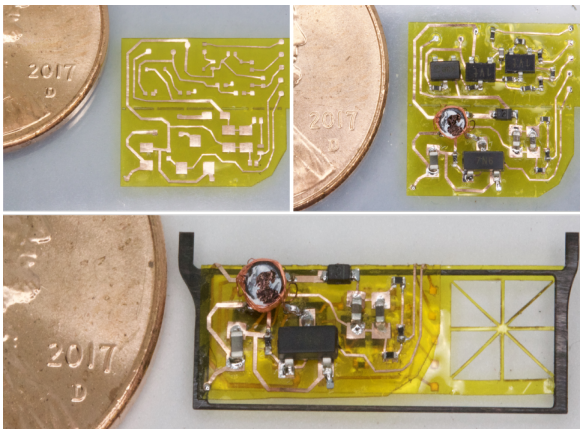

Fig. 6: PEU at several stages in the circuit fabrication process. Top left: bare unpopulated circuit. Top right: circuit populated with components including coupled inductor. Bottom: Assembled PEU with boost converter and driver, ready to mount to robot.

the total 5.2 V to below 4 V at which the boost converter stops functioning in empirical evaluation. Perhaps even more important than their inability to support sustained flight though is their combined weight of 96 mg which is greater than the weight of the entire boost converter.

A. *Optical Wireless Power Transfer*

Since on-board energy storage cannot meet the requirements for flight, we look to wireless power technologies instead. A practical wireless power solution for an insect scale robot must meet two criteria: 1) it must be able to deliver the 250 mW of power required for flight, and 2) it should have an operating range that allows for flight. Near field magnetic induction can provide efficient power delivery and have been demonstrated for walking robots [9], however its range is fundamentally constrained to tens of centimeters. Far-field microwave approaches (e.g., Wi-Fi) can operate at longer ranges but suffers from efficiencies less than 1% due to RF path loss [14]. We instead select an optical approach as lasers provide a collimated beam with high power density that can be harvested by photovoltaic (PV) cells with conversion efficiencies of over 20%.

Our laser power delivery system consists of a 976 nm laser source and a photovoltaic (PV) cell. For our laser source we use the MHGoPower LSM-010 976 nm laser source capable of providing 10 W of optical power. We connect the fiber output to a collimator (Thor Labs F220FC-980) to produce a beam in free space. An ideal laser should produce a perfect collimated beam that does not diverge in space, however the internal focusing optics of this laser and the use of multi-mode fiber causes measurable beam divergence in space.

Unlike typical PV cells designed to harvest broad spectrum solar energy, our system should be optimized for a single wavelength and high power densities. We therefore select a vertical multi-junction PV cell (MH GoPower 5S0303.4) [15] which consists of serially interconnected p-n junctions bonded together to form a small PV array with low series resistance that performs well under high intensity light [15]. The PV cell measures 2.88 mm x 2.95 mm and weighs 8 mg with an additional 5 mg of wires. This is well within the size and weight constraints of our Robofly. We find experimentally that at intensities up to 20 W/cm^2 the cells achieve maximum power output when operating at 8.8 V with efficiencies of up to 40% for short pulses.

While a power source for liftoff only requires a limited range, we note that laser power beaming can be extended to longer ranges. For example, our laser can deliver sufficient power to the Robofly up to ranges of 1.23 m indoors. This range is not fundamentally limited, but rather determined by the beam divergence and output power of our specific laser source. At ranges beyond 1.23 m, our beam expands to a point where insufficient power is available over the small area of cell. Thus, we can in principle achieve tens of meters of range using commercially available lasers with higher output power or a more collimated beam.

While lasers are capable of powering the Robofly, their use raises other practical questions as well. First, to maintain flight, the laser must track the Robofly. Although tracking is beyond the scope of this work, potential solutions include using motion capture systems as demonstrated in [4] for robot control to track the position of the Robofly and direct the laser appropriately using a device like a galvo mirror. Additionally, we can simplify this problem by placing the laser on a ceiling or floor requiring it to move along only 2 axes. Another alternative to vision based approaches is to

use optical feedback from a device like a retroreflector. By placing a light weight retroreflector on the Robofly, we can use an additional laser to verify alignment to the robot. Such tracking systems could be attached to fixed or moving chase vehicles acting as laser power base stations.

Second, 976 nm laser radiation at the levels required for flight are above safe exposure limits. While the area within the laser may not be safe, we can exploit the fact that laser's power is highly focused, therefore guaranteeing that the unsafe areas are limited to the beam itself [16]. By using one of the tracking methods proposed above, we could recognize humans before they enter the beam to immediately turn off the laser source, thus complying with the exposure limits.

Component	Weight (mg)
DC-DC Converter & Driver Subtotal	**73.7**
Coupled Inductor	21
MOSFET	9.2
V_sCapacitor	2.6
Diode	1.5
Driver Transistors	17.5
Cu traces	6.3
Circuit Substrate	10.0
Assorted Resistors	0.4
Solder & Conductors	3.0
Carbon Fiber Frame	2.2
MCU Assembly	**17.5**
PV Cell & Leads	**13**
Robofly without PEU	**73**
Misc. Glue & Wiring	**13**
Total Robot Weight	**190**

TABLE I: Total weight of all robot components including body, power electronics, microcontroller, and PV cell.

VI. IMPLEMENTATION AND EVALUATION

We begin by describing the mechanical structure of our robofly MAV followed by a detailed description of our setup for flight experiments and discussion of results.

A. Robofly Design and Fabrication

The basic principle of the University of Washington (UW) Robofly design [17] inherits from [3]: a bimorph piezo cantilever actuator amplifies the small field-induced strains into relatively larger motions at the tip. This is further geometrically amplified by a transmission structure consisting of flexure joints to attain a $\approx 90^\circ$ stroke amplitude. The wing's angle of attack is allowed to rotate passively around a torsional spring consisting of a flexure at the base of the wing, resulting in a simple mechanism that produces insect-like wing kinematics. The airframe consists of a single folded structure made from laser micro-machined unidirectional carbon fiber composite bonded to polyimide flexural material. Slight changes to transmission/flexure geometry have greatly increased lift [10].

In addition to simplifying fabrication relative to [4], by employing only a single part for the airframe, our Robofly has a different arrangement of piezo actuators, that are oriented horizontally. This facilitates easy integration of electronics directly below, as shown in Fig. 7. The position of the electronics package was chosen to facilitate assembly and rework while avoiding adverse impacts on thrust and stability. The PV cell is positioned above the robot to achieve a direct line-of-sight path to the laser source. Without position tracking, liftoff will move the cell out of the laser beam and cut off power to the fly. We therefore assume a small flight altitude and position the cell at a height of 20 mm above the fly body. To drive the piezo bimorph to produce wing-flapping oscillations requires a roughly constant high-voltage bias signal, a ground signal, and an oscillating drive signal that is roughly sinusoidal, as shown in the top half of Fig. 3.

B. Setup and Takeoff Results

To demonstrate wireless liftoff capability, we position the fly at a distance of 1 m from the collimator output. With the beam divergence of the laser, this results in a 13 mm spot size at the PV cell which is more than sufficient to cover it. We design a $0.6 \times 0.75 \times 0.6$ m enclosure and use a series of 2 mirrors to achieve the 1 m distance and to align the beam on the cell. We program the microcontroller to flap both wings continuously at maximum possible amplitude at a frequency of 170 Hz using a single driver circuit to maximize lift. Because the fly is dynamically unstable and our goal is simply to demonstrate liftoff, we attach a carbon fiber rod across the base of the fly in order to minimize risk of structural damage during repeated experiments. We perform experiments by placing a digital camera inside the laser enclosure recording at a 240 Hz and apply short pulses from our laser power source.

Prior to performing flight experiments with the electronics attached, we verify that the fly is capable of liftoff when driven by a 190 Vpp sinusoid at 170 Hz with a 130 mg toothpick attached as a dummy load. Table. I shows the final weight of the power electronics amounts to 104 mg, which is well within this weight budget. We also verify the functionality of the full system by measuring the output of the electronics prior to final attachment on the fly while powered by the PV cell and driving the actual fly. We measure that the output of the PV cell is capable of providing over 250 mW to supply the power demands of the boost converter, drive circuit and microcontroller. Operating the boost converter at 150 kHz with a 6% duty cycle yields unloaded bias voltages of over 250 V as shown in Fig. 4. In this configuration, despite variation in the bias rail due to use of a smaller storage capacitor, the voltage difference between the bias and sinusoid is more than 170 V_{PP} at 170 Hz.

As seen in Fig. 1 and the supplementary video [18], we demonstrate a completely wireless RoboFly liftoff using only onboard electronics and wireless power transfer. We note that the altitude of the flight could be easily improved in future experiments. Specifically, the prototype fly shown in Fig. 7 includes a variety of fabrication errors and repairs which may have made flight even more difficult. Additionally, lighter components for the boost converter such as a sub milligram single chip voltage regulator to replace the multicomponent

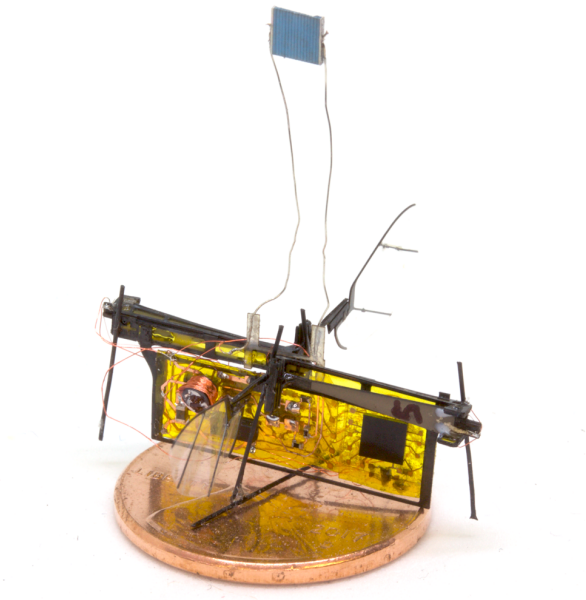

Fig. 7: Full insect scale robotic fly placed on a US penny for scale. The power electronics and microcontroller are below the robot and the PV cell is 20 mm above it.

shunt regulator used for the microcontroller, a lighter 5 mg MOSFET as well as laser micromachining to remove unpopulated areas of the circuit substrate would easily improve the payload margin. Performance could further be improved by reducing the power consumption of the micro-controller using low power optimizations on the chip or using alternative chips available in the same size or smaller thereby allowing a greater fraction of the total laser power to be delivered to the wings. These weight reductions could allow the use of a larger storage capacitor which would improve the boost converter and driver performance thereby increasing wing stroke amplitude and lift.

VII. RELATED WORK

Light weight robotic flight. Our work traces its lineage to the Berkeley Micromechanical Flying Insect project (MFI) to produce a honeybee sized flying robot. [2]. The MFI approach differed from a similar but parallel attempt, the mesicopter, that took a more traditional approach of rotors and electromagnetic motors [19], which achieved lift greater than weight in a larger, 3 g, 3 cm quad-rotor design. Fearing's piezo-and-wing approach, however, allowed for a much smaller package because electrostatic forces (piezo) scale downward more favorably in terms of efficiency and power density than magnetic forces (motor) [7]. The piezo approach first yielded lift greater than weight in $\approx$ 100 mg robot by Wood [3]. Since that time, subsequent advances derived from that basic approach [4][6] have required both power and computation to be supplied from offboard resources and supplied through a tiny wire tether. A recent work achieved successful lift-off along vertical guides [20] using electromagnetic actuation of a very similar flapping-wing insect-scale robot. Due to the dependence on high electrical current to generate a magnetic field, this approach requires roughly five times more power at 1.2 mW.

All other known demonstrations of wirelessly powered flight are either passive mechanical or magnetic designs which preclude useful autonomous application, or are substantially heavier. Purely mechanical demonstrations include a rubber-band powered butterfly with a comparable weight to our vehicle at 390 mg [21], and a 100 mg, 1 cm paper cone powered by external subwoofer [22]. [23] demonstrates a passive 5 mg flying machine using anisotropic magnetic structure in an alternating external magnetic field to flap wings. All electrically-powered robots are at least an order of magnitude heavier, including a 2.1 g jellyfish robot [24], the Delfy Micro at 3 g [25], the Piccolissimo at 2.5 g [26], and the nano hummingbird at 19 g [27]. Because the power required by a flying robot scales closely with its weight, lighter robots may make use of a greater diversity of power sources, some of which are too small to power larger robots.

Boost converter design. Prior works have proposed a variety of boost converter designs for MAVs using bimorph actuators. [28] proposed transformer based designs, however following [29], works have focused on coupled inductor designs. [30] and [12] have focused on combining custom controller ICs with coupled inductor circuits implemented off chip. However, control functionality for these converter designs can be implemented on micro-controllers of similar size and weight that are already heavily optimized for power and performance. Further, the weight of the converter circuit is dominated by the inductor. Thus, we focus on an off-the-shelf design that allows for faster prototyping and flexibility. Our topology and inductor fabrication method is similar to [11] which uses a bobbin and custom cut E-cores of similar size, however we do not implement energy recovery in order to reduce weight. While our design leverages these proven topologies, our circuit fabrication technique allows us to reduce weight. Most importantly, in contrast to prior work we demonstrate the first boost converter system and a laser based wireless power system, fully integrated into an MAV and demonstrate that it provides an output capable of liftoff.

Laser power beaming. Prior works have successfully demonstrated wirelessly powered robots [9] utilizing near field power transfer. However these robots are not capable of flight and the power transfer technique is physically limited to close operational range. In the realm of wirelessly powered aircraft, WiBotic is developing solutions for near field charging of drones [31], however as previously explained the weight constraints of our MAV make onboard energy storage such as rechargeable batteries infeasible.

Battery-free solutions such as the NASA Armstrong project demonstrates laser power transfer by manually directing a 1 kW laser at a 300 g fixed wing aircraft propelled by a 6 W motor [32]. More recently LaserMotive has demonstrated a laser power transfer to a quad rotor aircraft [33]. While these systems demonstrate wireless power transfer using lasers, we focus on aerial vehicles that are orders of magnitude smaller. Additionally, due to their higher weight

capacity and use of standard propulsion methods such as motors, these aircraft can use standard electronics components and circuit manufacturing techniques to drive their motors. In contrast wirelessly powering an MAV requires the power electronics introduced in this paper to take the raw output of the PV cell and convert it to the drive signal required by the actuators. Moreover, from a practical perspective the relatively low power requirements of insect scale robots allow the use of comparatively lower power lasers.

VIII. CONCLUSION

This paper presents a significant milestone towards the achievement of flight autonomy for honeybee-sized insect-scale robots, demonstrating a wireless takeoff. Specifically, we present the lightest wireless robotic flight to date by showing liftoff of a 190 mg robot. We demonstrate the first power electronics package fully integrated into a functional aerial robot and fabricated by a unique application of laser micro-machining techniques for fast-turnaround circuit fabrication. We also successfully demonstrate optical wireless power transfer sufficient to run the power electronics and onboard microcontroller.

This work serves as a platform for enabling a multitude of new research directions advancing MAVs closer to the vision of autonomous flight. The integration of an onboard microcontroller presents the opportunity to add sensing and communication capabilities which is a necessity for enabling onboard control and achieving extended stable flight. Laser based power for insect scale aerial robots also opens multiple research directions for extended flight including tracking, extending range, and laser-based communication.

ACKNOWLEDGEMENTS

The authors would like to thank Noah Jafferis for insightful discussions about how to increase lift.

REFERENCES

[1] R. A. Brooks and A. M. Flynn, "Fast, cheap, and out of control: A robot invasion of the solar system," *Journal of the British Interplanetary Society*, vol. 42, pp. 478–485, 1989.

[2] R. Fearing, K. Chiang, M. Dickinson, D. Pick, M. Sitti, and J. Yan, "Wing transmission for a micromechanical flying insect," in *Robotics and Automation (ICRA), 2000 IEEE Int. Conf.* IEEE, 2000.

[3] R. J. Wood, "The first takeoff of a biologically inspired at-scale robotic insect," *IEEE Trans. Robotics*, vol. 24, no. 2, pp. 341–347, 2008.

[4] K. Y. Ma, P. Chirarattananon, S. B. Fuller, and R. J. Wood, "Controlled flight of a biologically inspired, insect-scale robot," *Science*, vol. 340, no. 6132, pp. 603–607, 2013.

[5] S. B. Fuller, M. Karpelson, A. Censi, K. Y. Ma, and R. J. Wood, "Controlling free flight of a robotic fly using an onboard vision sensor inspired by insect ocelli," *Journal of The Royal Society Interface*, vol. 11, no. 97, p. 20140281, 2014.

[6] M. A. Graule, P. Chirarattananon, S. B. Fuller, N. T. Jafferis, K. Y. Ma, M. Spenko, R. Kornbluh, and R. J. Wood, "Perching and takeoff of a robotic insect on overhangs using switchable electrostatic adhesion," *Science*, vol. 352, no. 6288, pp. 978–982, 2016.

[7] W. S. N. Trimmer, "Microbots and micromechanical systems," *Sensors and Actuators*, vol. 19, pp. 267–287, 1989.

[8] R. J. Wood, B. Finio, M. Karpelson, K. Ma, N. O. Pérez-Arancibia, P. S. Sreetharan, H. Tanaka, and J. P. Whitney, "Progress on "pico" air vehicles," *Int. J. Robotics Research*, no. 11, 2012.

[9] M. Karpelson, B. H. Waters, B. Goldberg, B. Mahoney, O. Ozcan, A. Baisch, P. M. Meyitang, J. R. Smith, and R. J. Wood, "A wirelessly powered, biologically inspired ambulatory microrobot," in *2014 IEEE International Conference on Robotics and Automation (ICRA)*, May 2014, pp. 2384–2391.

[10] N. T. Jafferis, M. A. Graule, and R. J. Wood, "Non-linear resonance modeling and system design improvements for underactuated flapping-wing vehicles," in *2016 IEEE International Conference on Robotics and Automation (ICRA)*. IEEE, 2016, pp. 3234–3241.

[11] M. Karpelson, G.-Y. Wei, and R. J. Wood, "Driving high voltage piezoelectric actuators in microrobotic applications," *Sensors and Actuators A: Physical*, vol. 176, pp. 78 – 89, 2012.

[12] M. Lok, E. F. Helbling, X. Zhang, R. Wood, D. Brooks, and G. Y. Wei, "A low mass power electronics unit to drive piezoelectric actuators for flying microrobots," *IEEE Transactions on Power Electronics*, vol. PP, no. 99, pp. 1–1, 2017.

[13] S. I. Inc., "Low esr, low leak current chip-type edlc cpx3225a752d," 2016. [Online]. Available: http://www.sii.co.jp/en/me/datasheets/chip-capacitor/cpx3225a752d/

[14] V. Talla, B. Kellogg, B. Ransford, S. Naderiparizi, S. Gollakota, and J. R. Smith, "Powering the next billion devices with wi-fi," *ACM CoNEXT '15*.

[15] M. Perales, M.-h. Yang, C.-l. Wu, C.-w. Hsu, W.-s. Chao, K.-h. Chen, and T. Zahuranec, "Characterization of high performance silicon-based vmj pv cells for laser power transmission applications," in *Proc. of SPIE Vol*, vol. 9733, 2016, pp. 97 330U–1.

[16] V. Iyer, E. Bayati, R. Nandakumar, A. Majumdar, and S. Gollakota, "Charging a smartphone across a room using lasers," *IMWUT 2017*.

[17] Y. Chukewad, A. Singh, and S. B. Fuller, "A robot fly composed of actuator units folded from a single laminate sheet capable of flight, landing, and ground locomotion," in *Robotics and Automation (ICRA), IEEE Int. Conf.*, 2018, (under review).

[18] "Autonomous Insect Robotics Laboratory," 2018. [Online]. Available: http://depts.washington.edu/airlab/ICRA2018-1996.html

[19] I. Kroo and P. Kunz, "Development of the mesicopter: A miniature autonomous rotorcraft," in *American Helicopter Society (AHS) Vertical Lift Aircraft Design Conference, San Francisco, CA*, 2000.

[20] Y. Zou, W. Zhang, and Z. Zhang, "Liftoff of an electromagnetically driven insect-inspired flapping-wing robot," *IEEE Transactions on Robotics*, vol. 32, no. 5, pp. 1285–1289, Oct 2016.

[21] H. Tanaka and I. Shimoyama, "Forward flight of swallowtail butterfly with simple flapping motion." *Bioinspiration & biomimetics*, vol. 5, no. 2, p. 026003, Jun 2010.

[22] B. Liu, L. Ristroph, A. Weathers, S. Childress, and J. Zhang, "Intrinsic stability of a body hovering in an oscillating airflow," *Physical Review Letters*, vol. 108, no. 6, p. 068103, 2012.

[23] K. I. Arai, W. Sugawara, K. Ishiyama, T. Honda, and M. Yamaguchi, "Fabrication of small flying machines using magnetic thin films," *IEEE Transactions on Magnetics*, vol. 31, no. 6, pp. 3758–3760, Nov 1995.

[24] L. Ristroph and S. Childress, "Stable hovering of a jellyfish-like flying machine," *Journal of The Royal Society Interface*, no. 92, 2014.

[25] G. De Croon, K. De Clercq, R. Ruijsink, B. Remes, and C. De Wagter, "Design, aerodynamics, and vision-based control of the delfly," *International Journal of Micro Air Vehicles*, vol. 1, no. 2, pp. 71–97, 2009.

[26] M. Piccoli and M. Yim, "Piccolissimo: The smallest micro aerial vehicle," in *Robotics and Automation (ICRA), 2017 IEEE International Conference on*. IEEE, 2017, pp. 3328–3333.

[27] M. Keennon, K. Klingebiel, H. Won, and A. Andriukov, "Development of the nano hummingbird: A tailless flapping wing micro air vehicle," in *AIAA Aerospace Sciences Meeting*. Reston, VA: AIAA, 9–12 January 2012, pp. 1–24.

[28] E. Steltz, M. Seeman, S. Avadhanula, and R. S. Fearing, "Power electronics design choice for piezoelectric microrobots," in *Intelligent Robots and Systems, 2006 IEEE/RSJ International Conference on*. IEEE, 2006, pp. 1322–1328.

[29] M. Karpelson, G.-Y. Wei, and R. J. Wood, "Milligram-scale high-voltage power electronics for piezoelectric microrobots," in *Robotics and Automation, 2009. ICRA'09. IEEE International Conference on*. IEEE, 2009, pp. 2217–2224.

[30] S. Chaput, M. Renaud, R. Meingan, and J. F. Pratte, "A 3.7 v to 200 v highly integrated dc-dc converter with 70.4mems applications," in *2014 IEEE 12th International New Circuits and Systems Conference (NEWCAS)*, June 2014, pp. 381–384.

[31] "Wibotic," 2017. [Online]. Available: http://www.wibotic.com/

[32] NASA, "Laser power for uavs," 2004.

[33] T. J. Nugent, Jr. and J. T. Kare, "Laser power beaming for defense and security applications," pp. 804 514–804 514–8, 2011. [Online]. Available: http://dx.doi.org/10.1117/12.886169